Using Droplets of Nematic Liquid Crystal To Probe the Microscopic and Mesoscopic Structure of Organic Surfaces

Vinay K. Gupta† and Nicholas L. Abbott*,‡

Department of Chemical Engineering, University of Illinois, Urbana-Champaign, Illinois 61801, and Department of Chemical Engineering, University of Wisconsin—Madison, 1415 Engineering Drive, Madison, Wisconsin 53706

Received December 31, 1998. In Final Form: June 18, 1999

We report a simple and general procedure that uses nematic liquid crystals (NLCs) to probe the structure of organic surfaces prepared by molecular self-assembly. The procedure involves placement of a submillimeter-sized droplet of NLC on the surface of a self-assembled monolayer (SAM) of organic molecules and observation of the droplet under illumination with polarized light. Because NLCs are optically anisotropic, polarized light permits characterization of the distortion of the NLC within the droplet, which we demonstrate here to reflect the structure of surfaces on spatial scales that range from the molecular to the mesoscopic. We demonstrate the use of droplets of NLCs (i) to probe the molecular-level structure (Ångstrom-scale) of surfaces by distinguishing between SAMs formed from odd or even chain-length alkanethiols or SAMs coadsorbed from mixtures of long and short alkanethiols; (ii) to probe the nanometer-scale texture of polycrystalline films of gold used to support SAMs, including gold substrates prepared by oblique deposition from a vapor of gold; (iii) to image the micrometer-scale structure of SAMs patterned by using microcontact printing; and (iv) to follow, *in situ*, reactions on surfaces, using as an example the displacement of a SAM formed from $CH_3(CH_2)_6SH$ by $CH_3(CH_2)_{15}SH$ dissolved into the NLC. Because either reflection or transmission polarization microscopy can be used to image the NLC drops, this method permits characterization of monolayers of organic molecules on both transparent and opaque substrates. To clarify the relationship between the optical appearance of the NLC droplets, the distortions of NLCs within the droplets, and the orientations of NLCs near SAMs, we report numerical simulations of droplets of NLCs supported on surfaces and calculations of the optical textures of these droplets.

I. Introduction

Studies of the interactions between liquid crystals (LCs) and the surfaces of solids have now spanned nearly a century.[1−9] Although much of the recent interest in LCs has been driven by their widespread use in optical displays, studies at the beginning of this century focused on the use of LCs to determine the symmetry of surfaces of cleaved inorganic crystals.[3,4,6] In this article, we extend these early ideas by using droplets of nematic liquid crystals (NLCs) to characterize the structure of organic surfaces prepared through molecular self-assembly.[10]

Numerous previous studies have demonstrated that liquids can form the basis of analytical methods for the characterization of surfaces.[11−17] For example, measurements of contact angles of polar and nonpolar isotropic liquids have been widely used to explore the contributions of polar and dispersion forces to the excess free energy of surfaces.[11−17] Patterns formed by condensation of droplets of liquids on surfaces—so-called "breath figures"—have also been used to image the lateral structure of surfaces on micrometer and larger scales.[18,19] Although the microscopic balance of forces governing the condensation and wetting of liquid on surfaces is not understood completely, these methods are widely used for the characterization of organic surfaces, including surfaces formed by molecular self-assembly (e.g., self-assembled monolayers, SAMs). Contact angles of liquids supported on SAMs, for example, have been demonstrated to reflect both the structure of the outer few Angstroms[11,12] of each SAM as well as long-range (>10 Å) dispersion forces that act between polarizable metallic substrates (e.g., gold) supporting SAMs and the overlying liquid.[20] In this article, we demonstrate that drops of NLCs placed on surfaces can also form the basis of simple and general methods to characterize the structure of SAMs and metallic substrates used to support SAMs. We demonstrate that droplets of NLCs can be used to distinguish between surfaces that differ in their molecular and meso-scale structure. Droplets of NLCs are also shown to provide the basis of straight-

* To whom correspondence should be addressed. E-mail: abbott@engr.wisc.edu.
† University of Illinois.
‡ University of Wisconsin-Madison.

(1) Jerome, B. *Rep. Prog. Phys.* **1991**, *54*, 391.
(2) Cognard, J. *Mol. Cryst. Liq. Cryst., Suppl. Ser.* **1982**, *1*, 1.
(3) Gaubert, P. *C. R. Acad. Sci. Paris* **1938**, *206*, 62.
(4) Grandjean, F. *Bull. Soc. Fr. Mineral.* **1916**, *39*, 164.
(5) Maugin, C. *Bull. Soc. Fr. Mineral.* **1911**, *34*, 71.
(6) Maugin, C. *C. R. Acad. Sci. Paris* **1913**, *156*, 1246.
(7) Bahadur, B. *Liquid Crystals*: *Applications and Uses*; World Scientific: Singapore, 1990.
(8) Chandrasekhar, S. *Liquid Crystals*; Cambridge University Press: Cambridge, 1977.
(9) de Gennes, P. G.; Prost, J. *The Physics of Liquid Crystals*; Clarendon Press: Oxford, 1993.
(10) Ulman, A. *Chem. Rev.* **1996**, *96*, 1533.
(11) Bain, C. D.; Whitesides, G. M. *J. Am. Chem. Soc.* **1988**, *110*, 3665.
(12) Bain, C. D.; Whitesides, G. M. *J. Am. Chem. Soc.* **1988**, *110*, 5897.
(13) Adamson, A. W.; Gast, A. P. *Physical Chemistry of Surfaces*; Wiley: New York, 1997.
(14) Chen, L.; Helm, C. A.; Israelachvili, J. N. *J. Phys. Chem.* **1991**, *95*, 10736.
(15) de Gennes, P. G. *Rev. Mod. Phys.* **1985**, *57*, 827.
(16) Ondarcuhu, T.; Veyssie, M. *Nature* **1991**, *452*, 418.
(17) Young, T. *R. Soc. London* **1805**, *95*, 65.
(18) Lopez, G. P.; Biebuyck, H. A.; Frisbie, C. D.; Whitesides, G. M. *Science* **1993**, *260*, 647.
(19) Kane, T. E.; Angelico, V. J.; Wysocki, V. H. *Anal. Chem.* **1994**, *66*, 3733.
(20) Miller, W. J.; Abbott, N. L. *Langmuir* **1997**, *13*, 7106.
(21) Berggren, E.; Zannoni, C.; Chiccoli, C.; Pasini, P.; Semeria, F. *Phys. Rev. E*: *Stat. Phys. Plasmas, Fluids, Relat. Interdiscip. Top.* **1994**, *50*, 2929.
(22) Chiccoli, C.; Pasini, P.; Semeria, F.; Zannoni, C. *Phys. Lett. A* **1990**, *150*, 311.

10.1021/la981780g CCC: $18.00
Published on Web 08/27/1999

forward procedures that permit the imaging of surfaces on micrometer scales.

Previous studies of droplets of NLCs have focused on polymer-dispersed liquid crystals (PDLCs).[21−26] These composite materials consist of micrometer-sized droplets of a NLC dispersed in an isotropic polymeric matrix. The optical characteristics (scattering of light) of these composite materials depend strongly on the orientations of the NLCs within the droplets, which, in turn, are determined by a balance of effects. These effects include the elastic energy stored in distorted states (bend, twist, and splay) of the NLC, short-ranged interactions between the NLC and the surrounding polymer matrix (the so-called anchoring energy), and any externally applied (electric or magnetic) fields.[24] Here we report on the relationship between distortions formed within droplets of NLCs supported on surfaces (in the absence of applied fields) and properties of the underlying surfaces.

By using nematic and smectic LCs confined between two planar surfaces (i.e., a LC cell), our previous work has demonstrated that LCs can be used (i) to distinguish between surfaces that appear to be the same when characterized by measurements of both advancing and receding contact angles[27] and (ii) to optically image events at surfaces such as specific binding between biological molecules (e.g., antibody−antigen recognition).[28] In contrast to these previous studies based on LC cells, here we move to investigations based on the use of droplets of NLCs for two broad reasons. First, whereas procedures based on confinement of NLCs between two planar surfaces require the assembly of LC cells for each measurement, placement of a drop of LC on a surface is both fast and simple to perform. Procedures based on droplets of LCs can also be used to characterize the surfaces of substrates that are optically opaque. Second, because the distortions formed by LCs within droplets do reflect a balance of elastic and surface effects (see above), we believe this geometry may ultimately lead to methods that will permit ranking of the relative strength of anchoring of LCs at surfaces by using the optical appearance of droplets. In contrast, LCs confined to uniformly oriented LC cells assume the same "easy direction" for both strong and weak anchoring at surfaces. Contact angles are widely used for the characterization of surfaces because the value of the contact angle provides a useful relative index with which to rank surfaces (the absolute values are often not interpreted).

The investigation we report herein has two parts. First, we demonstrate that distortions do form within droplets of NLC placed on surfaces in ways that are characteristic of the structure of these surfaces on length scales that range from the molecular scale (Angstroms) to the mesoscopic (micrometers). Second, we use numerical simulations to understand how surfaces induce distortions within droplets of NLCs.

We chose SAMs formed from *n*-alkanethiols [$CH_3(CH_2)_n$-SH] supported on films of gold as model surfaces. Extensive characterization of these SAMs by a variety of analytical techniques has shown that the sulfur headgroups of the alkanethiols chemisorb onto the gold surface to form a densely packed $(\sqrt{3} \times \sqrt{3})R30°$ lattice that is commensurate with the underlying Au(111).[29] The alkyl chains of long-chain alkanethiols organize into nearly all-*trans* configurations that tilt by ∼30° from the normal of the surface; variations in the twist angles of neighboring chains gives rise to a $c(4 \times 2)$ superlattice.[30,31] The structure of these surfaces can be manipulated on length scales that range from the molecular scale (Ångstroms) to the mesoscopic (micrometers) by using one of several approaches. First, by using alkanethiols with odd and even chain lengths, surfaces that present methyl groups with two distinct orientations can be prepared.[32] Second, by using mixtures of long and short alkanethiols, surfaces presenting loosely packed long chains that protrude from a densely packed sublayer of chains can be prepared.[33] Third, oblique deposition of films of gold can be used to introduce a subtle level of anisotropy on length scales comparable with the size of the gold grains (∼20 nm).[34,35] Fourth, patterning of SAMs by using microcontact printing permits the preparation of surfaces that possess lateral structure on micrometer length scales.[36]

To simulate the distortions formed by NLCs within droplets, we use a cubic lattice model and minimize the energy at each site by evaluating nearest-neighbor interactions. Although simulations of distortions of NLC within droplets have been reported[21−23,25] for droplets dispersed in an isotropic polymeric matrix, the case of a droplet of NLC placed on a solid surface differs from that of microdroplets dispersed in an isotropic matrix (such as in PDLCs) for two reasons. First, a droplet of NLC on a solid substrate has two interfaces: the air−NLC interface and the solid−NLC interface. The excess surface free energy of the droplet, therefore, is determined by the anchoring of the NLC at both interfaces; in polymer-dispersed LC droplets, in contrast, only one interface exists (the polymer−NLC interface). Second, previous studies of droplets have focused on spherically symmetric droplets; this symmetry is broken when droplets rest on the planar surfaces of solids. To our knowledge, only one study[37] has investigated this geometry: a NLC droplet was simulated on the surface of liquid water. The results of our simulations provide the orientational structure within a droplet of NLC resting with a prescribed contact angle on the surface of a solid. We then transform the simulated distortion of the NLC into polarized light images and use the (simulated) polarized light images to interpret our

(23) Chiccoli, C.; Pasini, P.; Semeria, F.; Zannoni, C. *Mol. Cryst. Liq. Cryst.* **1992**, *212*, 197.
(24) Drzaic, P. S. *Liquid Crystal Dispersions*; World Scientific: River Edge, NJ, 1995.
(25) Kilian, A. *Liq. Cryst.* **1993**, *14*, 1189.
(26) Ondris-Crawford, R.; Boyko, E. P.; Wagner, B. G.; Erdmann, J. H.; Zumer, S.; Doane, J. W. *J. Appl. Phys.* **1991**, *69*, 6380.
(27) Gupta, V. K.; Miller, W. J.; Pike, C. L.; Abbott, N. L. *Chem. Mater.* **1996**, *8*, 1366.
(28) Gupta, V. K.; Skaife, J. J.; Dubrovsky, T.; Abbott, N. L. *Science* **1998**, *279*, 2077.
(29) Chidsey, C. E. D.; Bertozzi, C. R.; Putvinski, T. M.; Mujsce, A. M. *J. Am. Chem. Soc.* **1990**, *112*, 4301.
(30) Camillone, N.; Chidsey, C. E. D.; Liu, G.; Scoles, G. *J. Chem. Phys.* **1993**, *98*, 4234.
(31) Poirier, G. E.; Tarlov, M. *Langmuir* **1994**, *10*, 2853.
(32) Nuzzo, R. G.; Dubois, L. H.; Allara, D. L. *J. Am. Chem. Soc.* **1990**, *112*, 558.
(33) Bain, C. D.; Whitesides, G. M. *J. Am. Chem. Soc.* **1989**, *111*, 7164.
(34) Gupta, V. K.; Abbott, N. L. *Langmuir* **1996**, *12*, 2587.
(35) Skaife and Abbott used atomic force microscopy (AFM) to characterize quantitatively structural anisotropy within ultrathin (thickness of ∼10 nm) *obliquely* deposited films of gold (Skaife, J. J.; Abbott, N. L. *Chem. Mater.* **1999**, *11*, 612−623). These gold films are formed of grains with lateral dimensions of ∼20 nm and radii of curvatures of ∼50 nm. Although anisotropy within these films cannot be seen unambiguously by visual inspection of AFM images, a quantitative analysis of the AFM profiles shows a subtle level of anisotropy on wavelengths comparable with the size of the gold grains (∼20 nm). Their analysis revealed the root-mean-square (RMS) slope of the surface topography to be greater by approximately a degree in the direction parallel to the direction of deposition of the gold as compared with the perpendicular direction. They also find the RMS curvature of the grains of gold to be greatest in a direction parallel to deposition.
(36) Kumar, A.; Abbott, N. L.; Kim, E.; Biebuyck, H. A.; Whitesides, G. M. *Acc. Chem. Res.* **1995**, *28*, 219.
(37) Press: M. J.; Arrott, A. S. *Phys. Rev. Lett.* **1974**, *33*, 403.

experimental observations. The results of the simulation suggest approaches that may permit parameters such as the anchoring energy of a NLC on a surface to be obtained from analyses of the optical images of drops of NLC placed on surfaces.

II. Methods

Experimental. Self-assembled monolayers were formed from *n*-alkanethiols [$CH_3(CH_2)_{n-1}SH$, $4 < n < 17$] on the surface of thin (~100 Å thickness), semitransparent films of polycrystalline gold that were prepared by electron beam evaporation. All gold films (unless otherwise specified) were prepared by using oblique deposition of the gold. A detailed description of the procedure used to deposit the gold has been reported previously.[34,35] The SAMs were prepared by immersing films of gold in solutions of alkanethiols using either ethanol or isooctane as the solvent. Patterned SAMs were prepared by using the technique of microcontact printing with an elastomeric stamp formed from poly(dimethylsiloxane) (PDMS).[36]

The optical textures formed by droplets of NLC of 4-cyano-4′-pentylbiphenyl (5CB) supported on SAMs were measured by using the following procedure. First, we heated 5CB within a hypodermic syringe to a temperature that was greater than its nematic-to-isotropic transition temperature (~34 °C). Second, a drop of the 5CB was dispensed from the syringe onto the surface of a SAM (warmed to ~36 °C by placement on a heated stage). The SAM supporting the droplet of 5CB was then transferred to a thermostated chamber mounted on a polarized light microscope and cooled to a temperature less than the nematic-to-isotropic transition temperature (typically ~30−32 °C). The optical appearance of the supported NLC drop was imaged by using Sony CCD camera and recorded on a computer using Media-grabber software (Rasterops Corp., CA).

Computational. The distortion of a NLC within a droplet supported on a SAM was simulated by extending the numerical approach reported by Windle and co-workers[38,39] to the geometry of a supported droplet. The shape of the droplet (Figure 1A) was described by a locus of points satisfying the equation[40]

$$x^2 + y^2 + K z = 1 \tag{1}$$

where K is a constant and the surface of the solid is defined by the plane at $z = 0$. By changing the value of K, the contact angle of the supported droplet can be specified. We did not use a hemispherical droplet because it corresponds to a rather unrealistic contact angle of 90°. In past work, we measured the contact angle of 5CB on a SAM formed from $CH_3(CH_2)_{15}SH$ to be about 57°. We used a value of K of ~1.5 in our simulations, which corresponds to a contact angle of ~54°.

The orientation of the NLC within the supported droplet is described by dividing the droplet into 51 × 51 × 18 cubic cells placed on a lattice with overall dimensions of 2 × 2 × 0.68. Each cell in the lattice defines a local volume element of the NLC (inset in Figure 1A) and a director (**n**) can be assigned to each cell. The excess free energy of NLC within a cell is defined by its interaction with the six nearest neighbors along the x, y, and z directions. Previous studies have made use of several different forms of the interaction between nearest neighbor cells.[38,39,41,42] The simulation described in this article is based on an algorithm proposed by Bedford and Windle.[38] The algorithm, which approximates the excess free energy in terms of the angular difference between the director of a central cell and the director of the nearest neighbor cells, has successfully modeled the microstructure of NLCs. In particular, for a three-dimensional

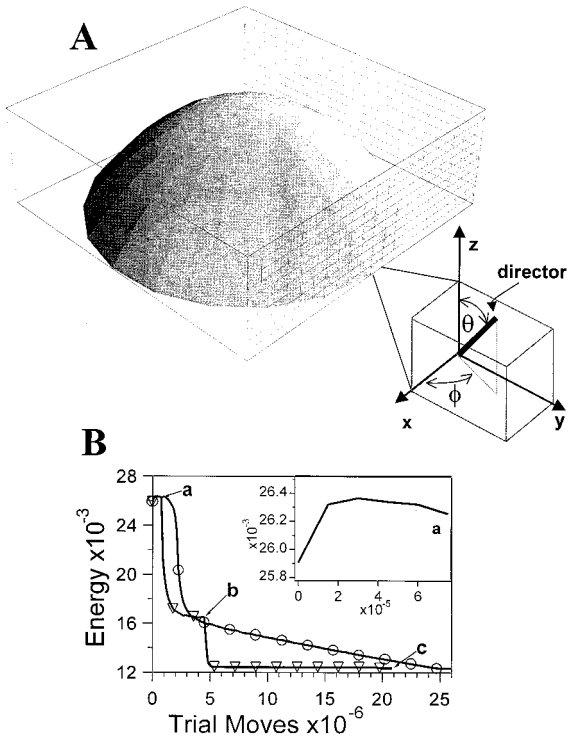

Figure 1. A, Schematic illustration of the lattice used to model a droplet of NLC supported on a surface. The inset shows a magnified view of a cubic cell of the lattice. The preferred orientation of the NLC in the cubic cell is given by the director and is specified by the angle of tilt (θ) and the azimuthal orientation (ϕ). B, Total energy (E) of a droplet of NLC as a function of the number of trial moves when the parameter α is decreased discretely (∇) or continuously (O) using a linear function. The inset shows a magnified view of the first 800 000 trial moves.

lattice, the excess free energy of a single cell E_j with a director defined by a unit vector $\mathbf{n_j}$ is given by

$$E_j = \sum_{i=1}^{6} |n_j \times n_i|^2 \tag{2}$$

The summation in eq 2 is performed over the six nearest neighbors in a cubic lattice where $\mathbf{n_i}$ is the unit vector describing the orientation of the director in each neighboring cell. Both $\mathbf{n_j}$ and $\mathbf{n_i}$ are defined by their local Euler angles (θ, ϕ), where θ is the angle **n** makes with the z-axis (angle of tilt) and ϕ is the angle **n** makes with the x-axis (azimuthal orientation). The total energy of N cells is given by

$$E = 0.5 \sum_{j=1}^{N} \sum_{i=1}^{6} |n_j \times n_i|^2 \tag{3}$$

where the numerical coefficient (0.5) corrects for double counting of cells.

Equations 2 and 3 are based on the assumption that elastic constants describing twist, splay, and bend distortions are equal in magnitude. Although this model is a simple one, the forms of eqs 2 and 3 do satisfy several constraints that describe properties typical of LC systems. Because the director is an apolar vector, the excess energy should remain unchanged upon substitution of **n** by −**n**; the expression for energy in eq 2 satisfies this criterion. Further, the excess energy described by this simple equation does drive the system toward an undistorted state. In the absence of surface effects, the global minimum of the energy E corresponds to a state in which the director is undistorted throughout the volume of the system. A more complete discussion of eq 2, and a comparison of eq 2 with other forms of the elastic energy, can be found elsewhere.[42] Although eq 2 is successful for low molar mass LCs, Hobdell and Windle[39] have shown that it does not

(38) Bedford, S. E.; Windle, A. H. *Liq. Cryst.* **1993**, *15*, 31.
(39) Hobdell, J.; Windle, A. *Liq. Cryst.* **1997**, *23*, 157.
(40) Several other equations can be used to represent the profile of the drop and to satisfy the criterion for the contact angle at the surface. For quantitative predictions, the drop profile that best captures the actual experimental profile should be used. The choice of the profile will depend on the interfacial tensions of the solid−liquid and the liquid−vapor interfaces as well as the effects of gravity. Our future work will explore the effects of drop shape and size using numerical simulations.
(41) Kimura, T.; Gray, D. G. *Macromolecules* **1993**, *26*, 3455.
(42) Assender, H. R.; Windle, A. H. *Macromolecules* **1994**, *27*, 3439.

capture saddle-splay distortion, and therefore, the approximation does not completely describe microstructures in polymeric LCs. For our purposes, eq 2 serves as a useful starting point to predict and interpret distortions formed within droplets of 5CB supported on surfaces.

We describe the influence of a supporting surface on the orientation of LC within a droplet by prescribing values for θ and ϕ within the cells of the lattice that lie at the surface of the substrate. For example, the value of θ within each cell at the supporting surface is given a value in the interval [0°, 90°], where 0° corresponds to homeotropic alignment (alignment of the director normal to the surface) and 90° corresponds to planar alignment (alignment of the director parallel to the surface). The effect of the surface on the azimuthal orientation ϕ of the LC is also included by specifying ϕ for each lattice cell at the surface. All the results presented in this article assume the orientation of the director at the free surface of the droplet to be normal to the curved interface. This corresponds to homeotropic anchoring of 5CB at its free surface.[43] When θ and ϕ at the surface of the droplet are fixed for all distortions of the LC within the droplet, the surface is said to exhibit "strong anchoring" with an infinite anchoring energy. In the numerical results presented here, we discuss only two cases: (i) strong anchoring at both the free surface of the droplet and the surface of the supporting substrate, and (ii) strong anchoring at the free surface with no constraint on the orientation of the director at the supporting substrate, i.e., a solid surface with zero anchoring energy. In future work, we plan to modify the simulations to describe the effects of "weak anchoring" at the solid surface.

To minimize the total energy of the droplet, we use a procedure similar to one proposed by Hobdell and Windle.[39] Cells of the lattice are selected at random within the droplet and a random trial orientation is generated within a cone-shaped region around the existing orientation of the director within the cell. A Metropolis algorithm is used to accept or reject the trial orientation.[44] If the energy of the trial orientation is lower than the original orientation, it is accepted. For trial orientations with energy higher than the original, the new trial orientation is accepted with a probability given by

$$P = \exp^{-\Delta E/\alpha} \tag{4}$$

where α is an arbitrary numerical parameter and ΔE is the change in energy caused by the trial move. The parameter α is used in two ways. First, α is set to a high value at the start of the simulation to randomize the orientation of the LC within the droplet. Second, α is slowly reduced to a small number to minimize the energy of the droplet yet prevent the system from getting trapped in local minima. As the system tends toward its minimum in energy, a high fraction of the trial orientations is rejected if the angular variation of the trial move is large. The angle for the cone-shaped trial region is reduced, therefore, using a procedure given by Allen and Tildesley[44] to keep the fraction of trial moves that are accepted a constant (i.e., maintain a constant acceptance ratio). Typically, each simulation involves $10-20 \times 10^6$ trial moves and is completed within an hour on a desktop computer (Dell, Pentium 233 MHz).

We calculated the polarized light images of the droplets by simulating the passage of monochromatic light through the droplet. The calculations were performed for incident light that was linearly polarized. The angular rotation and phase shifts of the polarized light were calculated by using a method described by Nicholson for a cubic lattice.[45] The phase shift of the light caused by optical retardation in each cell was calculated by assuming that the wavelength (λ) of the incident light is 633 nm and the ordinary (n_o) and extraordinary (n_e) refractive indices to be 1.5 and 1.7. These values correspond to the birefringence of 5CB at room temperature. For a ray of light propagating along the z-axis, the effective extraordinary index (n_{eff}) in each cell is calculated based on the local polar orientation (θ)

$$n_{eff}(\theta) = \frac{n_o n_e}{\sqrt{n_o^2 \sin^2\theta + n_e^2 \cos^2\theta}} \tag{5}$$

We evaluated the phase retardation of light transmitted through a cell with thickness d as

$$\delta = \frac{2\pi(n_{eff} - n_o)d}{\lambda} \tag{6}$$

Zero phase retardation ($n_{eff} = n_o$ and $\delta = 0$) occurs when the director in a cell lies perpendicular to the surface (i.e., $\theta = 0°$). The maximum phase retardation ($n_{eff} = n_e$) occurs when the director lies parallel to the surface (i.e., $\theta = 90°$).

The procedures we used to calculate the polarized light images are described in the Appendix. The simulated optical textures reported in this article were evaluated by assuming $d = 1\ \mu$m. The assumed value for the thickness of each cell (d) influences the order of retardation in the simulated texture but not the energy calculation. The effect of the value of d on the simulated optical textures is discussed under Results and Discussion.

III. Results and Discussion

Simulations of Director Profiles and Optical Textures. We first present the results of our numerical simulations of director profiles within droplets of NLCs because these results provide a framework within which to interpret the optical textures of droplets of LCs measured in our experiments. We have simulated five cases. Four of these cases correspond to "strong anchoring" and differ by the orientation imposed on the NLC at the surface of the substrate: (i) the NLC is anchored normally to the surface of the supporting solid ($\theta = 0°$, homeotropic anchoring); (ii) the NLC is anchored parallel to the surface of the supporting solid ($\theta = 90°$) and along a unique azimuthal direction (uniform, planar anchoring); (iii) the NLC is anchored parallel to the surface of the supporting solid ($\theta = 90°$) with a degenerate azimuthal orientation (nonuniform, planar anchoring); and (iv) the NLC is anchored with a tilt from the normal of the supporting solid (arbitrarily set to $\theta = 36°$) with a unique azimuthal direction in the plane of the surface (for example, along positive y-axis or $\phi = 90°$; uniform, tilted anchoring). The fifth case treats a droplet of NLC supported on a substrate that exerts no direct influence over the orientation of the NLC.

Figure 1B shows the profile of the total energy E during a simulation of a droplet of NLC that is anchored homeotropically at the surface of the solid. The first 200 000 steps correspond to a process of randomization of the director within the droplet. At the end of the initial increase in energy ("a" in Figure 1B), the orientation of the NLC within the drop is randomized (Figure 2A, E, and F). After the director is allowed to relax for approximately 5×10^6 iterations ("b" in Figure 1B), a substantial decrease in energy is observed and the director varies smoothly in space. The simulated optical image of the drop (Figure 2B) shows evidence of a cross at the center of the drop. After several million additional iterations ("c" in Figure 1B), the final state shown in Figure 2C is reached. Because the azimuthal orientation (ϕ) of the director in the final state is radially symmetric (Figures 2G and 2H), for cells lying along the $x-z$ plane and the $y-z$ plane, the projection of the director onto the $x-y$ plane is either parallel ($\phi = 0°$) or perpendicular ($\phi = 90°$) to the direction of polarization of the incident light (x-axis). The polarization of light transmitted through these regions of the droplet is, therefore, unchanged and thus the light is extinguished by the analyzer (causing dark brushes to appear along the x- and y-axes). In contrast, the director

(43) Sonin, A. A. *The Surface Physics of Liquid Crystals*; Gordon and Breach: Amsterdam, 1995.

(44) Allen, M. P.; Tildesley, D. J. *Computer Simulation of Liquids*; Clarendon Press: Oxford, 1987.

(45) Nicholson, T. M. *Mol. Cryst. Liq. Cryst.* **1989**, *177*, 163.

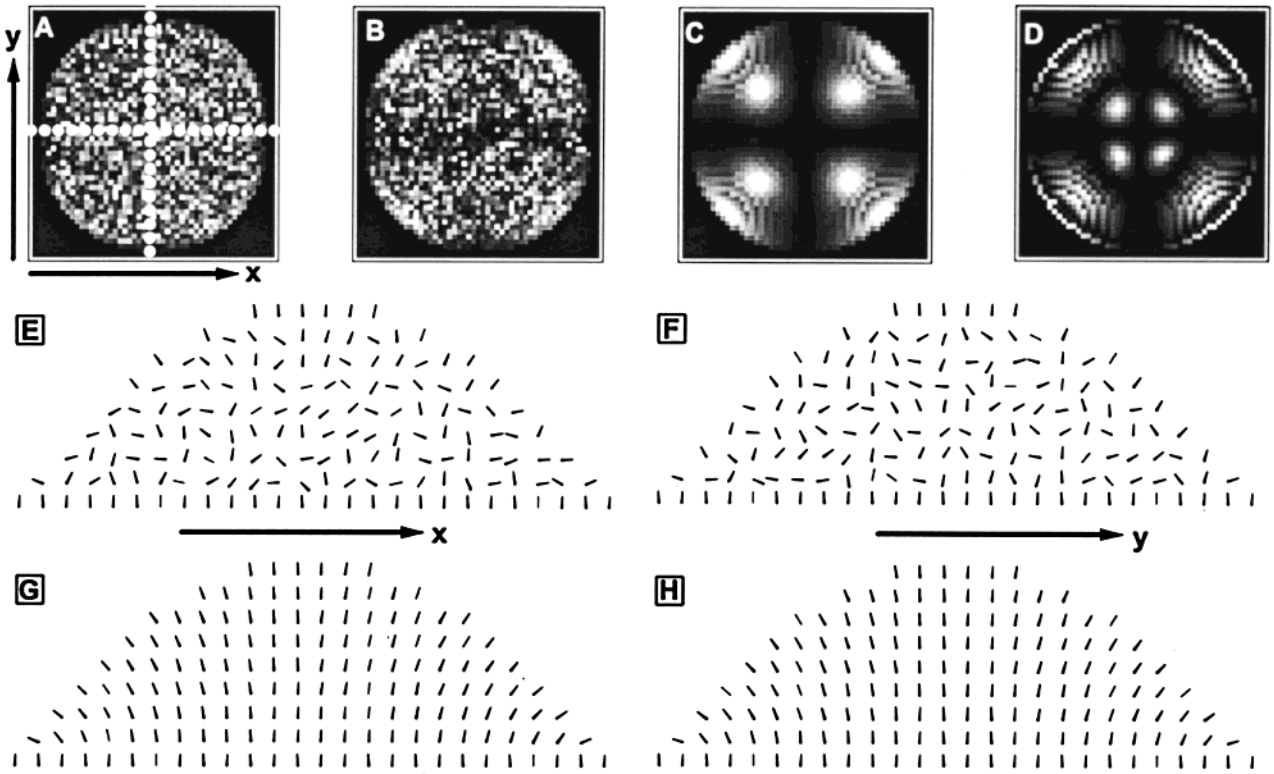

Figure 2. Simulated polarized light images of a NLC droplet resting on a surface with homeotropic boundary conditions. The droplet is centered at the origin and the images are simulated at different stages of the relaxation of the director within the droplet. Image A corresponds to stage a indicated in Figure 1B. The white dashed lines indicate projections of the $x-z$ and $y-z$ plane onto the $x-y$ plane. Images B and C correspond to b and c, respectively, indicated in Figure 1B. Image D shows the optical texture calculated using $d = 2\ \mu$m in the evaluation of the phase shift. The vector fields along the $x-z$ and $y-z$ planes are shown in images E and F and illustrate the orientational distribution of the director corresponding to A. The director field in G and H corresponds to the image shown in C. In the plots of the director field, only a fraction of the lattice cells are shown for clarity.

within all cells that lie between the $x-z$ and $y-z$ planes possess an azimuthal orientation described by a value of ϕ that lies between 0° and 90°: the change in polarization of light passing through these regions leads to the transmission of light through the analyzer. In contrast to the simulated images shown in Figures 2A−C, where phase shifts of the polarized light were calculated by assuming $d = 1\ \mu$m, higher order retardation is observed when $d = 2\ \mu$m (Figure 2D). In particular, a circular ring corresponding to the first-order black color is seen in Figure 2D.

Figure 3 shows where the surface has either no influence on the orientation of the director (Figures 3A−C) or causes planar anchoring of the LC without a preferred azimuthal orientation (Figure 3D). When no constraint is imposed on the orientation of the LC by the surface of the solid, the director tilts away from the normal to minimize distortion of the LC within the droplet (Figures 3A and 3B). The simulated polarized light image resembles the image shown in Figure 2C for homeotropic anchoring (a Maltese cross with four dark brushes). However, the dark circular rings at the center and edge of the droplet in Figure 3C indicate that even though $d = 1\ \mu$m, the net phase retardation experienced by the light in Figure 3C is much greater than that in Figure 2C. The greater retardation in Figure 3C than Figure 2C is caused by the large tilt of the director near the surface of the substrate in Figure 3C and its absence in the case of homeotropic anchoring. Figure 3D shows the simulated polarized light image where the NLC lies parallel to the surface of the supporting substrate ($\theta = 90°$) but has no preferred azimuthal orientation. The nonuniform anchoring of the LC on the surface of the substrate results in a wide

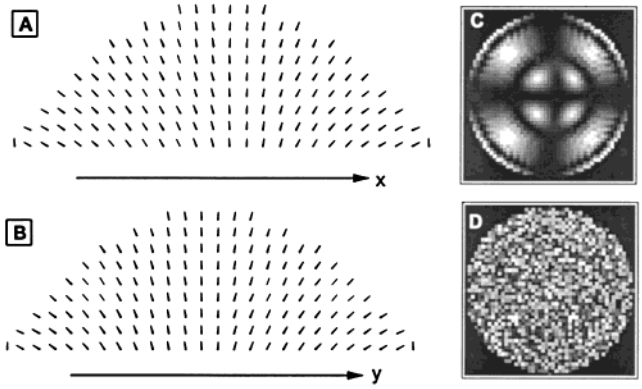

Figure 3. A−C, Simulated polarized light images of a NLC droplet resting on a surface that imposes no constraints on the orientation of the director. The director field is shown along the $x-z$ plane (A) and the $y-z$ plane (B), and the simulated polarized light image is shown in C. D, The simulated polarized light image of a droplet resting on a surface with strong anchoring conditions such that the director is constrained to lie parallel to the surface but not along a unique azimuthal direction (nonuniform planar anchoring).

distribution of orientations within the droplet and a complex and disordered optical texture.

Figures 4A−C show the results of a simulation for the case where the NLC lies parallel to the surface of the supporting substrate ($\theta = 90°$) and along a unique direction (y-axis, $\phi = 90°$). We can deduce the type of deformation within the droplet of NLC by looking at Figures 4A−C and by considering the orientation at the bottom and top surfaces of the drop (Figure 4D). First, all cells located within the $y-z$ plane contain a director with an azimuthal

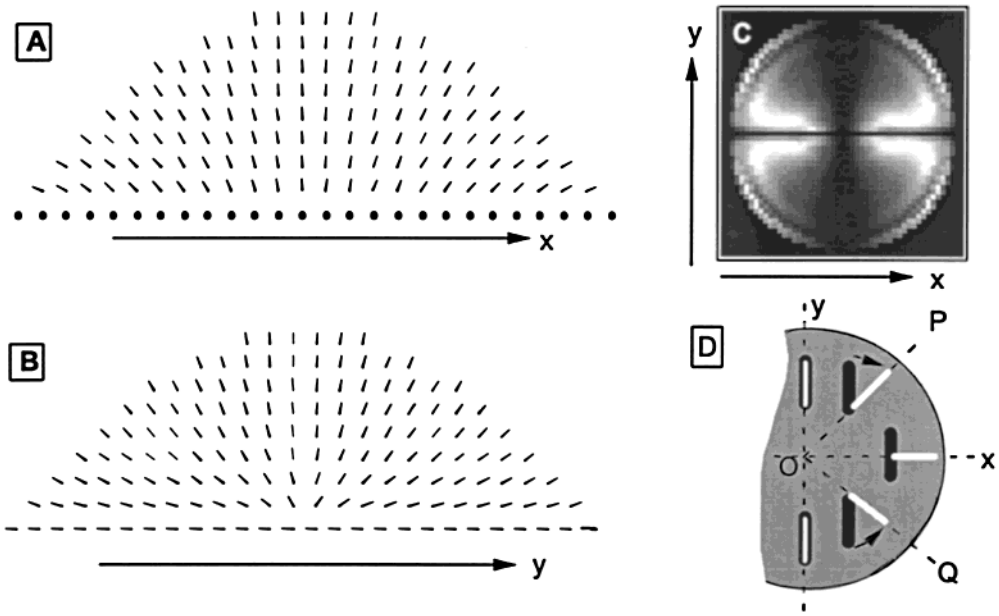

Figure 4. Simulated polarized light images of a droplet of NLC resting on a surface with planar boundary conditions ($\theta = 90°$, $\phi = 90°$). The director field is shown along the $x-z$ plane (A) and the $y-z$ plane (B), and the simulated polarized light image is shown in C. A schematic view of the drop projected onto the $x-y$ plane is shown in D. The black lines correspond to the orientation of the director on the surface of the substrate (along the y-axis; $\phi = 90°$), whereas white lines correspond the $x-y$ projection of the director at the free surface of the drop.

orientation that is parallel to the y-axis at the solid−LC interface (the black line) as well as at the air−drop interface (the white line). No azimuthal twist of the NLC is required to satisfy the two boundary conditions in this region of the droplet, and therefore, the polarization of light transmitted through this region is unchanged. This process gives rise to the dark brush (parallel to y-axis) that appears in the optical texture in Figure 4C. In contrast, the directors within cells located along a diagonal plane indicated by the line OP possess an azimuthal orientation at the surface of the supporting substrate (the black vector) that is along the y-axis and an azimuthal orientation at the free surface that is described by an angle $\phi = 45°$ (to have homeotropic anchoring at the free surface). Consequently, the azimuthal orientation of the director must twist clockwise by ϕ as it moves from the surface of the substrate to the free surface. In regions of the cell where the director is twisted, the polarization of the light transmitted through the droplet is rotated and thus some fraction of the light is transmitted through crossed analyzer in these regions. (The drop appears bright.) The angle of twist caused by these opposing boundary conditions reaches a maximum in the regions of the droplet contained within the $x-z$ plane. Because the direction of twist changes discontinuously on either side of the $x-z$ plane (clockwise above the x-axis shown in Figure 4D to counterclockwise below the x-axis shown in Figure 4D), a line defect appears parallel to the x-axis. This orientational discontinuity is clearly visible in the simulated director field shown in Figure 4A (the first and second row of vectors from the bottom) and appears as a dark line in the simulated image shown in Figure 4C. In experimental measurements, however, line defects scatter light and this process cannot be described by the Jones-matrix formalism (see Appendix). As shown below, the scattering of light causes a similar disclination line to be readily apparent within the experimentally observed optical textures.

Figures 5 shows where the NLC is anchored at the surface of the supporting substrate with a tilt of 36° from the normal. The direction of the tilt is along the positive y-axis (Figure 5A). Several features of the director profile and simulated optical texture seen in Figure 5 are similar to Figure 4. For example, because the director within cells contained in the $y-z$ plane are also oriented within the $y-z$ plane, the simulated optical texture in Figure 5C appears dark along the y-axis. In contrast to the case shown in Figure 4, however, the line discontinuity (corresponding to a reversal in the handedness of the twist) is no longer located along the x-axis but intersects the y-axis at a negative value (far left side of Figure 5A). Furthermore, in the simulated optical image (Figure 5C), extending from the broad dark brush along the y-axis are two small dark lobes which bulge out on the sides. An optical image such as Figure 5C would, therefore, lead us to infer that (i) the NLC is neither parallel or normal to the surface but tilted from the surface, (ii) the tilt is along an axis coincident with the central dark brush (here the y-axis), and (iii) the tilt is toward the direction opposite to the direction in which the dark lobes are displaced along the tilt axis.

Experimental Results. In previous studies based on LC cells (LC sandwiched between two planar substrates), we reported the orientation of nematic phases of 5CB on SAMs formed from n-alkanethiols [$CH_3(CH_2)_{n-1}SH$] to be parallel to the surfaces of the SAMs.[34,46−48] When SAMs formed from $CH_3(CH_2)_{n-1}SH$ were supported on films of gold deposited obliquely, the azimuthal orientation of the nematic phase of 5CB was parallel to the direction of deposition of the gold for even values of n and orthogonal to the direction of deposition for odd values of n.[34,49] We began our experimental investigation of the optical textures of droplets, therefore, by examining droplets of NLCs supported on the surfaces of SAMs formed from alkanethiols with either odd or even chain lengths and by comparing experimental textures to the simulated ones

(46) Gupta, V. K.; Abbott, N. L. *Science* **1997**, *276*, 1533.
(47) Miller, W. J.; Abbott, N. L.; Paul, J. D.; Prentiss, M. G. *Appl. Phys. Lett.* **1996**, *69*, 1852.
(48) Drawhorn, R. D.; Abbott, N. L. *J. Phys. Chem.* **1995**, *99*, 16511.
(49) Gupta, V. K.; Abbott, N. L. *Phys. Rev. E: Stat. Phys. Plasmas, Fluids, Relat. Interdiscip. Top.* **1996**, *54*, R4540.

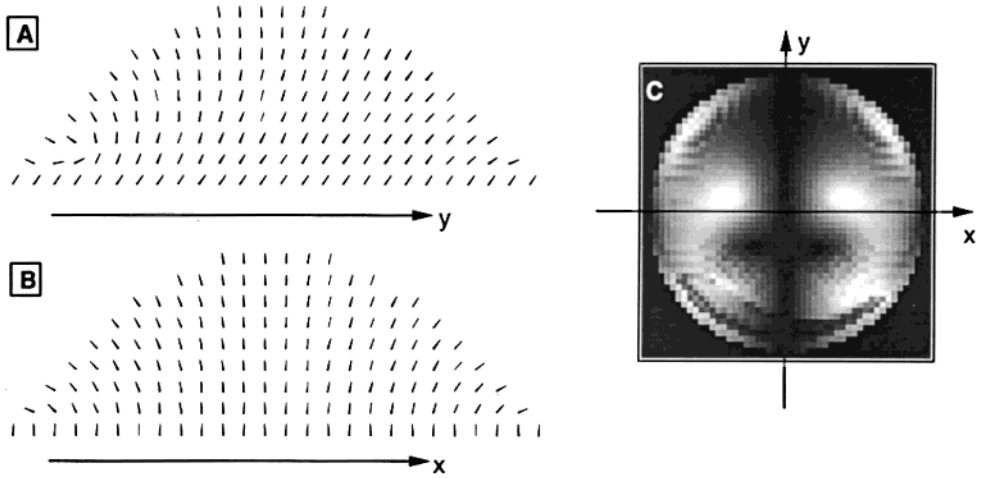

Figure 5. Simulated polarized light images of a droplet of NLC resting on a surface with uniformly tilted boundary conditions ($\theta = 36°$, $\phi = 90°$). The director field is shown along the $y-z$ plane (A) and the $x-z$ plane (B), and the simulated polarized light image is shown in C.

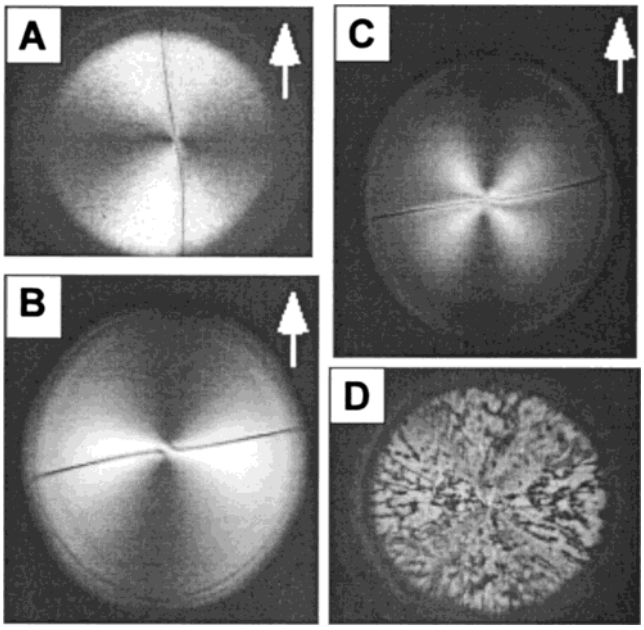

Figure 6. Transmission-polarized light image of a droplet of NLC resting on a SAM formed from $CH_3(CH_2)_{14}SH$ (A). The vertical arrow indicates the direction of deposition of the gold film. Polarized light images of a droplet of NLC observed under transmission (B) and reflection (C) when supported by a SAM formed from $CH_3(CH_2)_{15}SH$. D, Transmission polarized light image of a NLC droplet resting on a SAM formed from $CH_3(CH_2)_{15}SH$ on a gold film that was deposited uniformly. The horizontal dimensions of the images are 550 μm.

shown in Figure 4. Figure 6A shows a polarized light micrograph (transmission mode) of a droplet of 5CB placed on the surface of a SAM formed from $CH_3(CH_2)_{14}SH$. The thin, dark, threadlike structure observed in the optical micrograph is a disclination line. In this projection, the disclination line appears to pass through the core of a point defect at which two broad, dark brushes meet. This micrograph shares several features that are similar to the simulated optical textures where the NLC is anchored parallel to the surface of the substrate with a uniform azimuthal orientation (Figure 4): two broad, dark brushes were observed along one diameter of the drop and a line discontinuity was observed along the perpendicular diameter (Figure 4C). We conclude, therefore, that the micrograph shown in Figure 6A, corresponds to uniform, planar anchoring of the NLC on the surface of the SAM formed from $CH_3(CH_2)_{14}SH$. Because the computational results show the dark brushes to lie along a direction coincident with the preferred direction of azimuthal anchoring of the NLC on the surface of the substrate, we interpret the optical texture shown in Figure 6A to indicate that the preferred direction of alignment is perpendicular to the direction of deposition of gold. This result is consistent with the results of our previous studies using LC cells.[34,46,49]

We note that Yamaguchi and Sato have reported the optical texture of a droplet of NLC supported on the surface an obliquely deposited film of silicon oxide (SiO_x).[50] They, too, observe a line discontinuity in the optical texture. However, for reasons that are not understood by us, the images reported by Yamaguchi and Sato do not show the broad, dark brushes seen in Figures 4 and 6. One major difference between our experiments and those of Yamaguchi and Sato is that they used large drops (2−3 mm) whereas we have typically used droplets with sizes <500 μm. It is possible that the size of the droplets used by Yamaguchi and Sato were sufficiently large that the surfaces of the droplets did not control the orientation of the NLC near the center of the drop.

To test further whether the optical appearance of small droplets of NLC can be used to measure the azimuthal anchoring of NLCs on the surfaces of substrates, we deposited a droplet of 5CB onto a SAM formed from $CH_3(CH_2)_{15}SH$ (supported on obliquely deposited gold) and recorded its optical image (Figure 6B). The optical appearance of this droplet shared several features that were common to the droplet supported on the SAM formed from $CH_3(CH_2)_{14}SH$ (Figure 6A): a disclination line and pair of dark brushes were observed along perpendicular diameters. However, because the dark brushes in Figure 6B lie along the direction of deposition of gold, we conclude that the azimuthal anchoring of the LC on the SAM formed from $CH_3(CH_2)_{14}SH$ is orthogonal to that for the SAM formed from $CH_3(CH_2)_{14}SH$. The NLC drop therefore, can be used to distinguish between surfaces formed from either $CH_3(CH_2)_{14}SH$ or $CH_3(CH_2)_{15}SH$.

We also observed the droplet of NLC shown in Figure 6B (in transmission) by using reflection polarization microscopy (Figure 6C). The reflection micrograph also shows the disclination line and pair of dark brushes. Thus, droplets of NLCs can be used to study surfaces of optically

(50) Yamaguchi, R.; Sato, S. *Jpn. J. Appl. Phys., Part 2* **1996**, *35*, L117.

opaque substrates. This is not possible when the NLC is sandwiched between two planar, opaque surfaces.

Our previous studies have demonstrated the structure of films of gold on the 1- to 10-nm scale to be influenced by the manner of deposition of the gold.[34,35] To test whether a NLC drop can be used to distinguish between films of gold deposited with and without a preferred direction and angle of deposition, we observed the optical textures of droplets of NLCs supported on these two types of gold substrates. Figure 6D shows a polarized light micrograph of a droplet of 5CB placed on a SAM formed from $CH_3(CH_2)_{15}SH$ on a film of gold deposited without a preferred angle or direction of deposition. No disclination lines or dark brushes were observed in this micrograph, in contrast to the micrograph shown in Figure 6B (obliquely deposited substrate). We conclude that the NLC is anchored on the surface of the substrate without a preferred azimuthal orientation. A comparison of micrographs in Figures 6B and 6D demonstrates that droplets of NLCs can indeed be used to distinguish between variations in the structure of the gold surface caused by the manner of deposition of the gold.

By using LC cells, we have reported the orientations of nematic phases of 5CB on mixed SAMs formed by coadsorption of long and short alkanethiols to be either planar, tilted, or homeotropic, depending on the composition of the mixed SAM.[34,35,47,48] Our second set of experiments were designed, therefore, to investigate the optical textures of droplets of NLC supported on mixed SAMs to determine whether changes in the tilt of the NLC can be interpreted from the optical textures of droplets of NLCs. Figures 7A−B show optical micrographs (crossed polarizers, measured in transmission) of droplets of 5CB placed on mixed SAMs formed from $CH_3(CH_2)_6SH$ and $CH_3(CH_2)_{15}SH$. When supported on a mixed SAM prepared from a solution containing 0.4-mol fraction of $CH_3(CH_2)_6SH$ (Figure 7A), a dark brush with small "lobes" was observed in the optical micrograph of a droplet of NLC. In contrast, when a drop of 5CB was placed on the mixed SAM prepared from solution with 0.6-mol fraction of $CH_3(CH_2)_6SH$ (Figure 7B), a dark cross was observed at the center of the drop.

The experimentally observed optical image shown in Figure 7A resembles Figure 5C, and thus we conclude that the NLC is likely anchored with a tilt at the surface. Because NLCs typically possess unequal elastic constants, and because the mixed SAM may cause "weak anchoring" of the NLC, we do not expect our computations to match exactly the experimental image in Figure 7A. However, the conclusion of tilted anchoring of the NLC is consistent with results we obtained by using mixed SAMs of the same composition to form a LC cell.

Figure 7B resembles qualitatively the simulated structure shown in Figure 2C and indicates that the surface causes homeotropic anchoring. This is also consistent with results obtained by using a LC cell. We point out that the dark ring seen in the experimental image (Figure 7B) is not black but blue in color. The blue ring appears because white light was used to image the drops. The blue ring would not appear if monochromatic light had been used. No such ring is observed in simulated images because they were calculated assuming monochromatic light. In future work, we aim to extract more information from the experimental images by performing a full-color simulation of these textures and applying rules of color mixing.

Previous studies have shown that SAMs formed from short-chain alkanethiols can be displaced by long-chain alkanethiols by exposing the SAM to an environment (solution or vapor) containing the long-chain alkanethiols.[33] Herein we follow the displacement of SAMs formed from $CH_3(CH_2)_6SH$ by $CH_3(CH_2)_{15}SH$ by doping $CH_3(CH_2)_{15}SH$ into the NLC. Figure 8A shows an optical micrograph of a droplet of 5CB placed on a SAM formed from $CH_3(CH_2)_6SH$. Because the SAM is supported on obliquely deposited gold, a disclination line forms across the diameter of the drop when the drop cools from the isotropic phase to the nematic phase. The dark brushes indicate the preferred azimuthal orientation of the director. A droplet of 5CB doped with $CH_3(CH_2)_{15}SH$ (<0.05% weight fraction) placed on the same SAM was then imaged as a function of time. The sequence of textures in Figures 8B−J is the result of displacement of the SAM formed from $CH_3(CH_2)_6SH$ by $CH_3(CH_2)_{15}SH$ and consequent changes in anchoring of the NLC on the surface of the SAM. By comparing the optical micrographs in Figure 8 with the simulated optical textures in Figures 2−5, we can provide a partial account of the time-dependent changes in the structure of the droplets in Figure 8 and thus the anchoring of the NLC on the surface of the gold. The curved dark brushes in Figures 8B and 8C indicate that one of the first changes to occur to the structure of the droplet is the loss of the disclination line and formation of twist in the director field. The presence of the twist is consistent with the fact that the twist elastic constant for LCs is smaller than the splay or bend constants. It is therefore likely that the twist distortion is created because it causes minimal energetic cost. The absence of the disclination line suggests that displacement of a small fraction of the SAM formed from $CH_3(CH_2)_6SH$ by $CH_3(CH_2)_{15}SH$ likely causes a loss of the uniform azimuthal alignment of the LC that gives rises to the disclination line in Figure 8A. We propose, therefore, the first consequence of the displacement reaction to be a rotation of the azimuthal orientation of the LC at the surface of the SAM. The appearance of a ring at the perimeter of the droplet in Figure 8C, and its inward

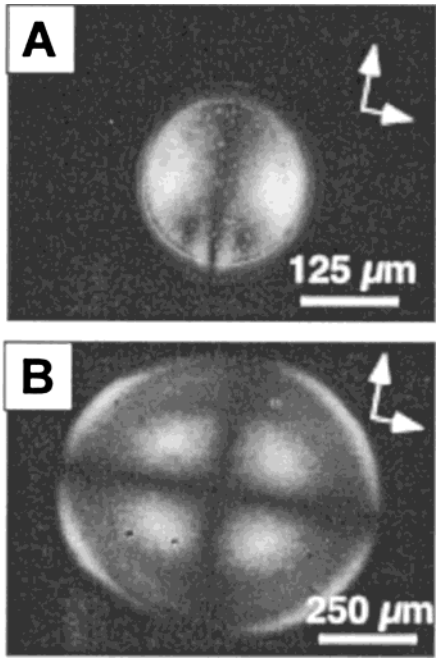

Figure 7. A, Transmission-polarized light image of a droplet of NLC resting on a mixed SAM formed from a solution containing a 0.4-mol fraction of $CH_3(CH_2)_6SH$ and 0.6-mol fraction of $CH_3(CH_2)_{15}SH$. B, Transmission-polarized light image of a droplet of NLC resting on a mixed SAM formed from a solution containing a 0.6-mol fraction $CH_3(CH_2)_6SH$ and 0.4-mol fraction $CH_3(CH_2)_{15}SH$. The arrows indicate the orientation of the crossed polarizers.

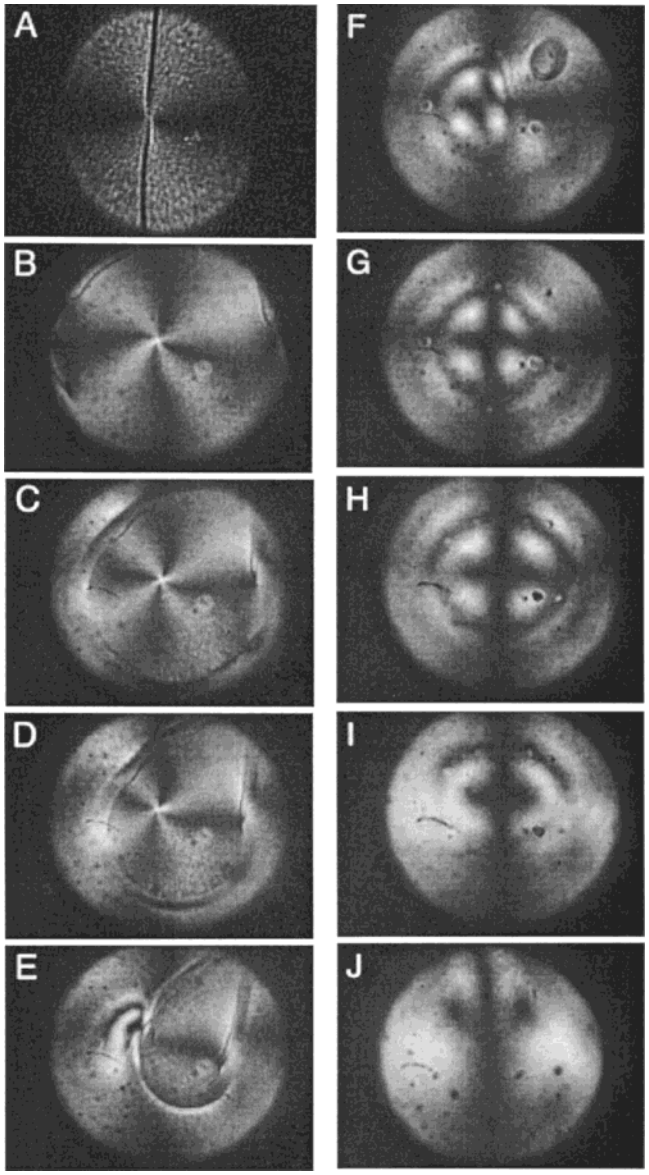

Figure 8. A, Transmission-polarized light image of a droplet of NLC [not doped with $CH_3(CH_2)_{15}SH$] resting on a SAM formed from $CH_3(CH_2)_6SH$. B−J, Transmission-polarized light images captured as a function of time for a droplet of NLC doped with $CH_3(CH_2)_{15}SH$ and supported on a SAM formed from $CH_3(CH_2)_6$-SH. Elapse times: B to F were recorded within the first 2 min of the reaction; G, ∼2 min; H, ∼22 min; I, ∼36 min; J, ∼103 min. The horizontal dimension of each image is 1100 μm.

growth in Figures 8D and E, indicates that a region exists outside of the ring in which the director reorients much faster than inside the ring, thereby causing an orientational discontinuity. Because regions outside the ring correspond to thin regions of the drop, it is plausible that the reorientation grows inward because the LC at the outer edge is closest to the free surface, i.e., the effect of the free surface is greatest. This interpretation is supported by the subsequent appearance of the droplet wherein a dark cross appears in the optical texture (Figure 8F−H). The transient image shown in Figure 8G resembles the simulated images shown in Figures 2D and 3C and indicates that displacement of $CH_3(CH_2)_6S$ in the SAM by $CH_3(CH_2)_{15}SH$ in the LC drop has caused one of two effects: (i) the mixed SAM formed by the displacement reaction causes the NLC to align homeotropically at the surface of the substrate (cf. Figure 2D) or, (ii) the mixed SAM formed by the displacement reaction exerts no influence over the orientation of the LC (cf. Figure 3C). Because most surfaces possess a finite anchoring energy and exert some influence on the orientation of a NLC, the second situation is less probable. Figures 8H and 8I show that further displacement of the SAM by $CH_3(CH_2)_{15}SH$ causes the dark cross to disappear. Comparison of the image in Figure 8I with the image in Figure 7A suggests that the NLC is uniformly tilted at the surface of the substrate: the tilt in Figures 8I−J appears to be in an azimuthal direction orthogonal to the direction in which the NLC was aligned on the SAM formed from $CH_3(CH_2)_6$-SH (cf. Figure 8A). The azimuthal alignment of the NLC after exchange is the same as the azimuthal orientation of the NLC supported on a SAM formed from $CH_3(CH_2)_{15}$-SH (cf. Figure 6B). That is, the azimuthal orientation of the NLC on the SAM appears dominated by the fraction of the SAM formed from $CH_3(CH_2)_{15}SH$.

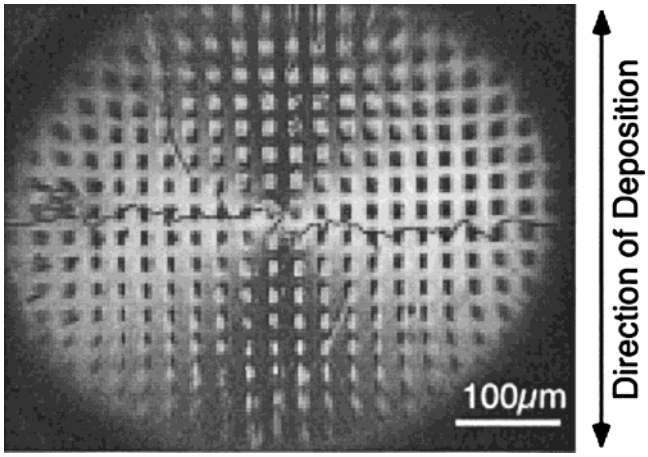

Figure 9. Transmission-polarized light image of a droplet of NLC resting on a film of gold patterned with a rectangular array of SAMs formed from $CH_3(CH_2)_{15}SH$ and $CH_3(CH_2)_{14}SH$. See text for description.

The rate of change of the optical texture of the droplet of NLC doped with $CH_3(CH_2)_{15}SH$ slowed substantially after a few minutes; after 2 days had elapsed, the optical texture of the droplet remained as shown in Figure 8J. In comparison, the texture of the undoped LC drop shown in Figure 8A remained unchanged throughout this study. Comparison of the optical texture in Figure 8J with Figure 6B indicated that complete displacement of $CH_3(CH_2)_6$-SH does not take place. Previous studies have used electrochemical methods to study exchange between ferrocene-terminated alkanethiols within SAMs supported on gold. These studies report an initial period of rapid exchange followed by long periods of little or no exchange between alkanethiols.[29,51] These studies also report that complete exchange of one species for another does not occur even at long times. Although our interpretation of the optical textures in Figure 8 is incomplete, further development of our computational model (to include finite anchoring energies) is ongoing. The results shown here, however, demonstrate that NLCs can form the basis of approaches that permit reactions on surfaces to be monitored *in situ*.

We have also demonstrated that droplets of NLCs can be used to image surfaces patterned with micrometer-scale features. Figure 9 shows an optical micrograph of a droplet of 5CB supported on a film of gold patterned with SAMs formed from $CH_3(CH_2)_{15}SH$ and $CH_3(CH_2)_{14}$-SH by using microcontact printing. The optical image in Figure 9 shows features that reflect the superposition of

(51) Collard, D. M.; Fox, M. A. *Langmuir* **1991**, *7*, 1192.

various effects. First, the two broad brushes along the *y*-axis and a disclination line orthogonal to the two brushes (along the *x*-axis) resemble the optical image of a droplet of NLC supported on a SAM formed from $CH_3(CH_2)_{15}SH$ (Figure 6B). Second, because the patterned SAMs orient 5CB in azimuthal directions that are orthogonal, the optical texture of the NLC drop forms an image of the patterned surface. The first feature of the optical texture likely reflects the fact that the SAM formed from $CH_3(CH_2)_{15}SH$ covers a larger fraction of the surface than the SAM formed from $CH_3(CH_2)_{14}SH$ and thus dominates the overall texture of the droplet. The second feature (the disclination line), however, differs from that shown in Figure 6B. The disclination line is thinner in Figure 9 than in Figure 6B, and it weaves across the surface in a manner that is influenced by the micrometer-scale structure of the patterned surface. In many regions of the patterned surface, it appears that the disclination line follows the boundary between regions of SAMs formed from $CH_3(CH_2)_{15}SH$ and $CH_3(CH_2)_{14}SH$.

Finally, we note that the rectangular pixels correspond to regions that are derivatized by $CH_3(CH_2)_{14}SH$. The pixels that lie within the dark brushes are bright, indicating that these regions correspond to a locally twisted NLC. In contrast, the pixels near the *x*-axis appear dark indicating that these regions correspond to a uniform alignment of the NLC. Thus, it appears that the local orientation of the LC follows the orientation that is dictated by the type of surface it encounters. By using drops with small dimensions, it will be possible to characterize surfaces patterned on the micrometer scale.

IV. Conclusions

We conclude that optical textures formed by submillimeter-sized droplets of NLCs placed on surfaces of solids can form the basis of convenient and simple procedures to image the structure of the surfaces. Because the distortion of the NLC within the droplet is determined by a balance of effects, including (i) the elastic deformation of the NLC, (ii) the anchoring of the NLC at the surface of the supporting solid, and (iii) the orientation of the NLC at the free surface of the NLC, observation of the distortion can be used to infer the orientation of the NLC at the surface of the solid. By using SAMs formed from alkanethiols on gold, we illustrate the use of droplets of NLCs for the characterization of the structure of these surfaces on spatial scales that range from the molecular to the mesoscopic. Because the NLC drops can be observed by using either transmission- or reflection-polarized light microscopy, this method can be used to study the surfaces of both transparent and opaque substrates. We also demonstrated the usefulness of simple computational models for providing qualitative interpretations of the structure of droplets of NLCs supported on surfaces.

The complexity of the procedures used in our investigations with liquid crystals are comparable to procedures used to characterize surfaces by contact angle measurements. In contrast to measurements of contact angles, however, the methods we report here are very effective in probing for the presence of in-plane anisotropy on surfaces. We believe this capability is a useful one because mechanical processes such as shear, flow, rubbing, and oblique deposition of materials from a vapor, all lead to various degrees of in-plane anisotropy. Although several of the optical texures formed by the LC droplets appear qualitatively similar, we believe refinement of the models reported in this article may lead to methods that permit quantitative interpretations of distortions observed within droplets of NLCs supported on surfaces. It is plausible that image analysis software could be written to compare quantitatively simulated and observed textures so as to back out the preferred orientation and anchoring energy of the liquid crystal at the surfaces of the system. Finally, we point out that the methods we report are promising ones for the imaging of micrometer-scale patterns on surfaces. This capability is not possible when using contact angles.

Acknowledgment. This research was supported, in part, by the Office of Naval Research (Presidential Early Career Award for Scientists and Engineers to N.L.A.) and the National Science Foundation (CAREER Program and DMR-9400354 to N.L.A.).

Appendix

This appendix presents a brief description of the evaluation of the polarized light image of a droplet of a NLC supported on a surface. The reader is directed to the following references for a more complete description.[26,45,52,53]

The optical texture is evaluated by assuming each vertical column of lattice cells (Figure 10) lies between crossed polarizers. The intensity of light that emerges from the column of cells is calculated. Light is incident on the bottom of the lattice and is polarized along the *x*-axis by the polarizer. The electric field of the incident light can be represented by

$$\begin{bmatrix} E_x \\ E_y \end{bmatrix} = \begin{bmatrix} E_o \exp(i\omega t) \\ 0 \end{bmatrix}$$

where E_x and E_y are the components of the electric field along the *x*- and *y*-axes, and ω is the frequency of light.

Because the droplets of NLCs used by us ($\sim$100$-$500 μm) are much larger than the wavelength of light, we use ray diagrams to describe the propagation of light. Within each cell, light propagates in two, mutually orthogonal directions that are parallel to the optical axis (extraordinary ray) and perpendicular to the optical axis (ordinary ray). The optical axis coincides with the local nematic director and is, for a general case, tilted from the surface ($\theta \neq 0°$). The propagation direction of the extraordinary ray, therefore, deviates from a rectilinear path. However, previous studies have shown that this deviation can be neglected when the ratio $(n_e - n_o)/n_o < 0.2$, which holds true for 5CB.[52] Optical effects such as deviations of the light ray caused by refraction and mixing of light rays caused by reflection will occur at the curved free surface of the droplet. These effects depend on the ratios $(n_e - n_o)/n_o$, $(n_o - n_{air})/n_o$.[26,52,53] We have neglected these effects in our calculations of the optical textures. They should be included in a quantitative analysis of optical textures, however.

With these approximations, the amplitudes of the electric fields along the two principal directions of cell 1 are then given by

$$E_{x1} = E_o \cos \phi_1 \exp[i(\omega t - \delta_1)]$$

$$E_{y1} = E_o \sin \phi_1 \exp(i\omega t)$$

where ϕ_1 is the azimuthal orientation in the first cell and δ_1 is the phase retardation in the first cell. The retardation of the phase depends on the tilt angle of the optical axis (θ) and is given by eq 5.

(52) Sherman, R. D. *Phys. Rev. A: At. Mol. Opt. Phys.* **1989**, *40*, 1591.
(53) Zumer, S. *Phys. Rev. A: At. Mol. Opt. Phys.* **1988**, *37*, 4006.

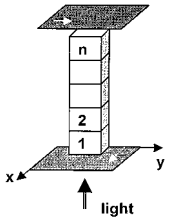

Figure 10. Schematic illustration of the column of *n* lattice cells placed between crossed polarizers (shaded) that is used to calculate the polarized light image of a droplet. See text for description.

The polarized light undergoes further rotation and phase shift in cell 2. The amplitudes of the electric field after the light emerges from cell 2 are given by

$$E_{x2} = \{E_{x1}\cos(\phi_2 - \phi_1) - E_{y1}\sin(\phi_2 - \phi_1)\}\exp(-i\delta_2)$$

$$E_{y2} = \{E_{x1}\sin(\phi_2 - \phi_1) + E_{y1}\cos(\phi_2 - \phi_1)$$

This calculation is repeated for all the cells in the column. The amplitudes of the electric field emerging from cell n are E_{xn} and E_{yn}. After passing through the analyzer, the intensity of light is given by E^2, where

$$E = E_{xn}\sin\phi_n - E_{yn}\cos\phi_n$$

The polarized light image is constructed from the computed value of the intensity.

LA981780G